

## Magnetocapacitance Effect in $\text{Gd}_x\text{Mn}_{1-x}\text{S}$

S. S. Aplesnin<sup>a,b\*</sup> and M. N. Sitnikov<sup>a</sup>

<sup>a</sup> Reshetnev Siberian State Aerospace University,  
pr. Krasnoyarskii Rabochii 31, Krasnoyarsk, 660014 Russia

<sup>b</sup> Kirensky Institute of Physics, Siberian Branch of the Russian Academy of Science,  
Akademgorodok 50, Krasnoyarsk, 660036 Russia

\* e-mail: apl@iph.krasn.ru

Received October 15, 2015

**Abstract**—The capacitance and dielectric loss tangent of  $\text{Gd}_x\text{Mn}_{1-x}\text{S}$  ( $x \leq 0.2$ ) solid solutions have been measured at a frequency of 10 kHz without magnetic field and in a magnetic field of 8 kOe in the temperature range of 90–450 K. An increase in the permittivity and a dielectric loss maximum have been detected in the low-temperature region. It has been found that the temperature of the maximum of the imaginary part of the permittivity shifts to higher temperatures with increasing concentration. The magnetocapacitance effect has been revealed for two compositions. The dielectric loss has been described in the Debye model with “freezing” dipole moments and in the orbital-charge ordering model.

DOI: 10.1134/S1063783416060032

Materials in which the interrelation of magnetic and electrical properties [1, 2], i.e., magnetoelectrics and multiferroics, are of interest from fundamental and applied points of view. Special attention is paid to materials exhibiting magnetoelectric properties in the region of room and higher temperatures in connection with practical applications in microelectronics for data recording and storage. Bismuth ferrite  $\text{BiFeO}_3$  is among such studied materials [3, 4]. The giant magnetocapacitance effect was observed in  $\text{LuFe}_2\text{O}_4$  at room temperature and was explained by charge fluctuations with various spins in  $\text{Fe}^{2+}$  and  $\text{Fe}^{3+}$  ions [5], due to the removal of the degeneracy between two types of charge orders by an external magnetic field. The linear magnetoelectric effect [6] can result from the dependence of orbital magnetic moments on polar distortions induced under an electric field, i.e., the so-called “ion–orbital” contribution to the magnetoelectric response [7].

Orbital degeneracy in manganese sulfide  $\text{MnS}$  can occur under  $n$ -type doping as a result of the substitution of the divalent manganese ion with trivalent gadolinium ion. Gadolinium sulfide  $\text{GdS}$  is a metal and has the same crystal and magnetic structure as that of the  $\text{MnS}$  semiconductor. Due to strong electron correlations in  $\text{MnS}$ , orbital ordering formation is possible. In  $\text{Gd}_x\text{Mn}_{1-x}\text{S}$  solid solutions, the magnetoresistance was detected in a wide temperature range, and the dependence of the magnetoresistance on the current and electric field was found [8].

However, the dc conductivity and permittivity are independent in some cases, and anomalies in one of

these quantities should not necessarily lead to anomalies in the other. When approaching the metal–insulator transition from the dielectric phase side, a decrease in the resistivity is accompanied by an increase in the permittivity, which was observed in some doped semiconductors [9]. The electronic permittivity contributes to the total permittivity via the interaction with ions which are displaced with the result of increasing polarizability [10].

In electrically inhomogeneous systems, the Maxwell–Wagner effect [11] and contact effects can lead to giant values of the permittivity and dielectric relaxation in the absence of dipolar relaxation [12]. The Maxwell–Wagner effect can also induce magnetocapacitance in the absence of the interaction between magnetic and electric subsystems under the condition of the magnetoresistance existences in a material [13]. Such effects clearly show that the existence of the magnetocapacitance is insufficient to attribute these compounds to multiferroics. At the same time, the magnetocapacitance without magnetoelectric coupling can be more practical for technological applications, since the far magnetic order existence is not necessary.

The objective of this study is to identify the magnetoelectric coupling mechanism in orbitally degenerate electronic states and to determine the relation between the magnetoresistance and magnetocapacitance in  $\text{Gd}_x\text{Mn}_{1-x}\text{S}$  solid solutions.

Synthesis of  $\text{Gd}_x\text{Mn}_{1-x}\text{S}$  solid solutions and their certification were previously described in detail in [14]. The samples are single-phase and have NaCl-

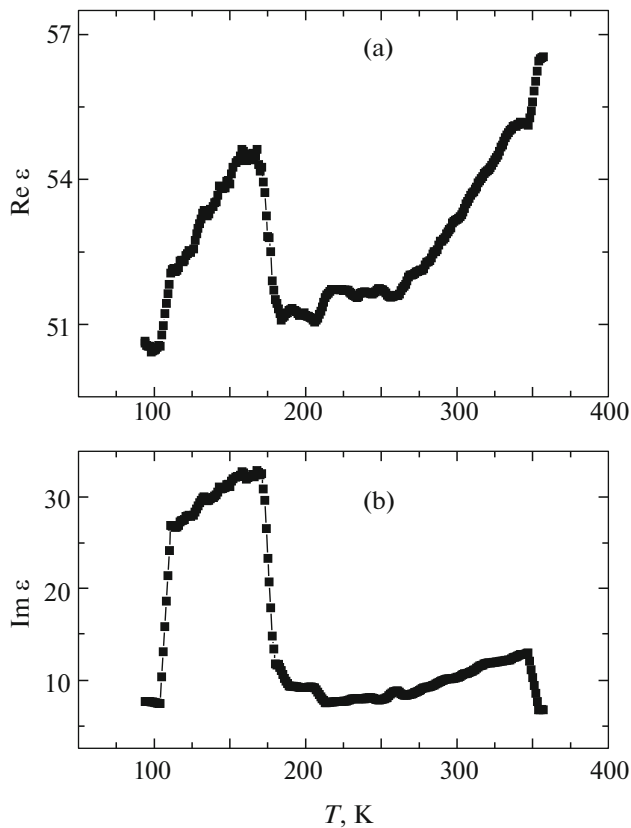


**Fig. 1.** (a) Real and (b) imaginary parts of the  $\text{Gd}_{0.04}\text{Mn}_{0.96}\text{S}$  permittivity at a frequency of 10 kHz as a function of temperature.

type crystal structure. The magnetic phase transition temperature of  $\text{Gd}_x\text{Mn}_{1-x}\text{S}$  monotonically decreases with increasing concentration from 150 to 120 K (at  $x = 0.2$ ). In the  $\text{Gd}_x\text{Mn}_{1-x}\text{S}$  solid solution with compositions  $x = 0.1, 0.15,$  and  $0.2$ , the magnetoresistance was determined at temperatures several times higher than the temperature of the transition to the magnetically ordered state. For all compositions, the semiconductor conductivity type with a small minimum in the high-temperature region was found. The increase in the resistivity in a magnetic field is associated with a decrease in the carrier mobility and is caused by orbital ordering of electrons with electric polarization formation.

The magnetocapacitance effect  $\delta\epsilon_H = (\epsilon(H, T) - \epsilon(0, T))/\epsilon(0, T)$  is determined by studying the complex permittivity. The spectral and temperature dependences of dielectric constants can be used to detect the dipole electric moment and to determine its characteristics, even in the case of the local dipole moment in small clusters without long-range order. The dielectric properties also reflect information about charge transport and charge ordering processes. The response of dielectric properties to a magnetic field makes it possible to identify the basic mecha-

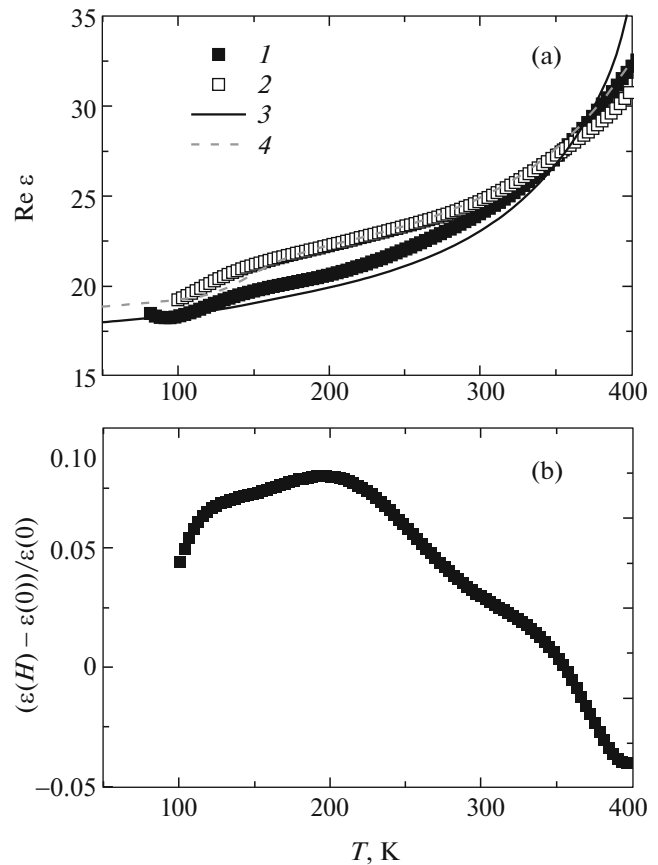


**Fig. 2.** (a) Real part of the permittivity of the  $\text{Gd}_{0.1}\text{Mn}_{0.9}\text{S}$  solid solution, measured at a frequency of 10 kHz (1) without field and (2) in the magnetic field  $H = 8$  kOe; approximating function (3) with the activation energy  $\Delta E = 0.069$  eV,  $T_c = 440$  K and (4)  $\Delta E = 0.086$  eV,  $T_c = 460$  K. (b) Relative variation of the permittivity in the field of 8 kOe as a function of temperature.

nisms controlling the behavior of dielectric and electrical transport properties.

The capacitance and dielectric loss tangent  $\tan\delta$  were measured using an AM-3028 component analyzer in the temperature range of 90–450 K without magnetic field and in the magnetic field  $H = 8$  kOe. The applied magnetic field was parallel to plane capacitor plates. Figure 1 shows the temperature dependences of the real  $\text{Re}\epsilon$  and imaginary  $\text{Im}\epsilon = \tan\delta\text{Re}\epsilon$  parts of the permittivity of the  $\text{Gd}_{0.04}\text{Mn}_{0.96}\text{S}$  sample. Sample heating causes a sharp increase in the dielectric loss, the imaginary part of the permittivity increases by a factor of 3, and the real part increases by 5% at  $T = 102$  K. As the temperature increases, the permittivity gradually increases and sharply decreases at  $T = 172$  K. A change in the  $\text{Gd}_{0.04}\text{Mn}_{0.96}\text{S}$  permittivity was not detected in a magnetic field within the experimental error of 1%. The sharp change in the permittivity is associated with lattice structure deformations reflected in the temperature dependence of

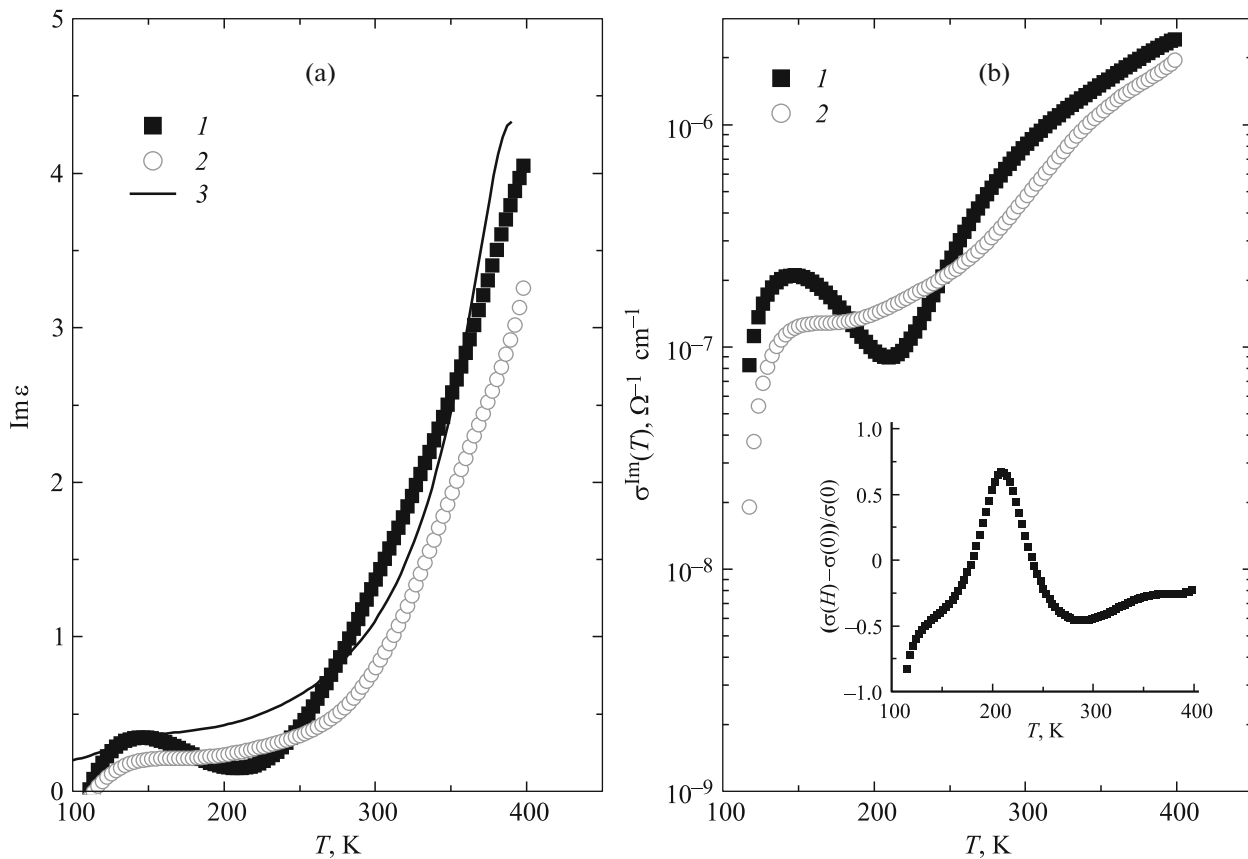


**Fig. 3.** (a) Imaginary part of the permittivity of the  $\text{Gd}_{0.1}\text{Mn}_{0.9}\text{S}$  solid solution, measured at a frequency of 10 kHz (1) without field and (2) in the magnetic field  $H = 8$  kOe, as a function of temperature. (3) Approximating function (3) with the activation energy  $\Delta E = 0.069$  eV,  $T_c = 440$  K. (b) Conductivity calculated using the relation  $\sigma^{\text{lm}} = \epsilon_0([\text{Im}(\epsilon(\omega))\omega]/4\pi)$  (1) without field and (2) in a magnetic field as a function of temperature. The inset shows the relative variation of the conductivity in a magnetic field as a function of temperature.

the lattice thermal expansion coefficient at  $T = 165$  K and in anomalies of the temperature dependence of the lattice parameter, shaped as a knee at this temperature in manganese sulfide [15].

As the gadolinium concentration increases, knees in the temperature dependence of the permittivity disappear. The real part  $\text{Re } \epsilon$  has an inflection point at  $T = 140$  K for the  $\text{Gd}_{0.1}\text{Mn}_{0.9}\text{S}$  composition, which is seen in Fig. 2. Upon further heating,  $\text{Re } \epsilon$  nonlinearly increases, as well as in the magnetic field  $H = 8$  kOe below a temperature of 357 K. Above this temperature, the permittivity decreases in the magnetic field. The relative variation of the permittivity  $\delta\epsilon_H = (\epsilon(H, T) - \epsilon(0, T))/\epsilon(0, T)$  in a magnetic field as a function of temperature is shown in Fig. 2b. The magnetocapacitance  $\delta\epsilon_H$  reaches a maximum of 8% at  $T = 200$  K.

The imaginary part of the permittivity for the  $\text{Gd}_{0.1}\text{Mn}_{0.9}\text{S}$  composition exhibits a maximum at  $T = 140$  K (Fig. 3a), which disappears in the magnetic field. The conductivity  $\sigma^{\text{lm}}$  and the related resistivity determined from the relation  $\rho = 4\pi/\epsilon_0[\text{Im}(\epsilon(\omega))\omega]$

are shown in Fig. 3b. The imaginary part of the permittivity decreases in the magnetic field, except for the temperature range of 180–240 K (Fig. 3a), and the dc magnetoresistance increases with temperature. The conductivity  $\sigma^{\text{lm}}(T)$  is not described within the Mott model with a variable hopping length, and its value is higher than the dc conductivity  $\sigma_{\text{st}}$  by five orders of magnitude (Fig. 4). The high value of  $\sigma^{\text{lm}}(T)$  is associated with a large contribution of lattice ion polarization to the imaginary part of the permittivity due to electron localization in potential wells.

Having divided all carriers into two groups, i.e., bound and free charges, we can write the medium permittivity as a sum of the lattice permittivity and the contribution of free carriers. Outside absorption bands, the imaginary part of the permittivity of (lattice) bound charges is usually neglected. An ensemble of carriers was considered as a sum of noninteracting particles. In semiconductors under  $n$ -type doping, electrons are delocalized in a certain region, the delocalization radius increases with temperature. Let us present the functional dependence in the form of the

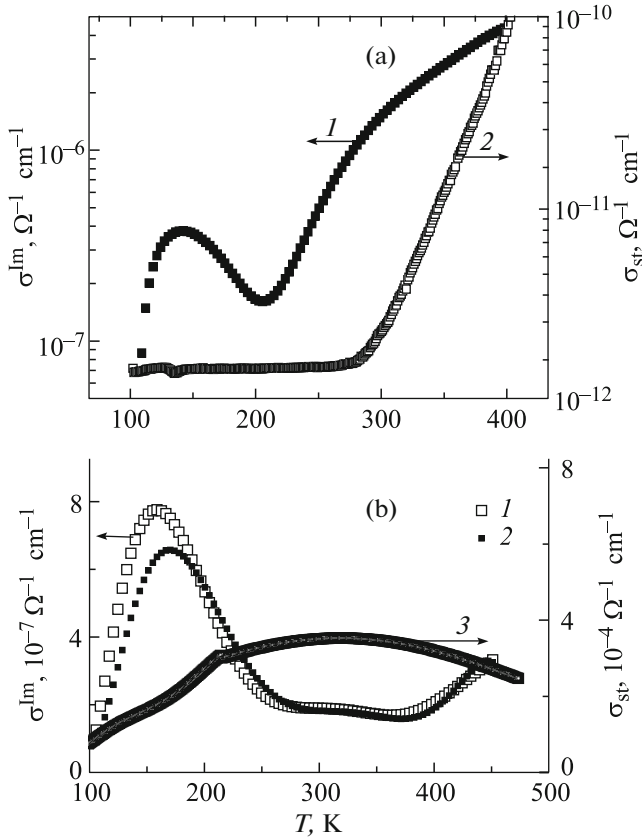


**Fig. 4.** (a) Conductivity (1) calculated from the relation  $\sigma^{\text{Im}} = \varepsilon_0[\text{Im}(\varepsilon(\omega))\omega]/4\pi$  and (2) measured at the direct current  $\sigma_{\text{st}}$  without magnetic field for the composition with  $x = 0.1$ , as a function of temperature. (b) Conductivity of the  $\text{Gd}_{0.2}\text{Mn}_{0.8}\text{S}$  solid solution, (1, 2) determined from the relation  $\sigma^{\text{Im}} = \varepsilon_0[\text{Im}(\varepsilon(\omega))\omega]/4\pi$  and (3) measured under a direct current  $\sigma_{\text{st}}$  (1, 3) without magnetic field and (2) in the magnetic field  $H = 8$  kOe as a function of temperature.

correlation radius  $\xi = A/(1 - T_c/T)$ , where  $T_c$  is the electron charge-ordering temperature at  $t_{2g}$ -orbitals. Localized electrons induce local ion displacements and lead to local polarization. The dielectric dynamic susceptibility of such a system is described in the Debye model. As the temperature is lowered, dipoles “freeze” at  $T_g$  due to the interaction between dipoles through the lattice. The dipole relaxation time is described by the Arrhenius function  $\tau_g = \tau_0 \exp(\Delta E/kT)$ , where  $\Delta E$  is the activation energy. The dielectric susceptibility can be written as

$$\begin{aligned} \text{Re}\chi/N &= \chi_{L0} + \chi_0/(1 + (\omega\tau_g)^2) \\ &+ \chi_0/(1 + (\omega\tau_c)^2) + B/(1 - T_c/T), \end{aligned} \quad (1a)$$

$$\begin{aligned} \text{Im}(\chi)/N &= \chi_0\omega\tau_g/(1 + (\omega\tau_g)^2) \\ &+ \chi_0\omega\tau_c/(1 + (\omega\tau_c)^2). \end{aligned} \quad (1b)$$

Here,  $\chi_{L0}$  is the temperature-independent contribution to the susceptibility,  $\chi_0$  is the static susceptibility of dipoles,  $B$  is a constant,  $\tau_g$  is the relaxation time of dipoles at a freezing temperature,  $\tau_c$  is the relaxation time of electric charges during the transition to orbital-charge ordering,  $\tau_c = A/\xi^z = A/(1 - T_c/T)^\nu$ , where  $z$  is the dynamic exponent and  $\nu$  is the correlation length exponent ( $\nu = 1$ ). We neglect the contribution of free carriers, since the conductivity  $\sigma^{\text{Im}}$  is higher than the dc conductivity by several orders of magnitude. The permittivity  $\varepsilon = 1 + \chi$  for the  $\text{Gd}_{0.1}\text{Mn}_{0.9}\text{S}$  composition is well described by the function

$$\begin{aligned} \text{Re}\varepsilon &= A/(1 + B \exp(2\Delta E/T)) \\ &+ C/[1 + (D/(1 - T/T_c)^2)^2] \\ &+ G/(1 - T/T_c) + \varepsilon_0 \end{aligned} \quad (2)$$

with parameters  $\Delta E = 0.069$  eV,  $T_c = 440$  K, and  $z = 2$ . In the magnetic field, the orbital ordering temperature increases to  $T_c = 460$  K. The imaginary part of the permittivity is qualitatively described by the function similar to (1b),

$$\begin{aligned} \text{Im}\varepsilon &= A_1 \exp(\Delta E/T)/(1 + B \exp(2\Delta E/T)) \\ &+ (C_1/(1 - T/T_c)^2) / [1 + (D/(1 - T/T_c)^2)^2] \end{aligned} \quad (3)$$

with the same constants as in Eq. (2), except for constants  $A_1$  and  $C_1$  in the numerator.

When the gadolinium ion concentration exceeds the percolation concentration  $x_c = 0.16$ , the resistivity varies within one order of magnitude and has a minimum at  $T = 325$  K in the temperature range of  $100 \text{ K} < T < 500 \text{ K}$  in the  $\text{Gd}_x\text{Mn}_{1-x}\text{S}$  solid solution. In the magnetic field, the resistivity also increases, and the minimum in the temperature dependence shifts to higher temperatures to  $T = 380$  K. The temperature dependence of the magnetoresistance changes sign from positive to negative at  $T = 320$  K, and the magnetoresistance tends to zero at a temperature of 475 K. For the composition with  $x = 0.2$ , the dc conductivity and the conductivity calculated from the imaginary permittivity  $\sigma = \varepsilon_0[\text{Im}(\varepsilon(\omega))\omega]/4\pi$  are qualitatively different (Fig. 4b). There are two conduction channels in this solid solution: over gadolinium ions and over the Mn–Gd ion interface. Therefore, the electronic contribution to the susceptibility should be added to Eq. (1).

Independently of the type (electrons or holes), free carriers decrease the real part of the permittivity. This decrease becomes more significant with increasing concentration and decreasing carrier effective mass. The decrease in the permittivity by free carriers is associated with their inductive contribution to the result of the interaction of the ac field with a material.

For the  $\text{Gd}_{0.2}\text{Mn}_{0.8}\text{S}$  composition, the permittivity is caused by localized electrons in the manganese ion sublattice and by conduction electrons in the gadolin-

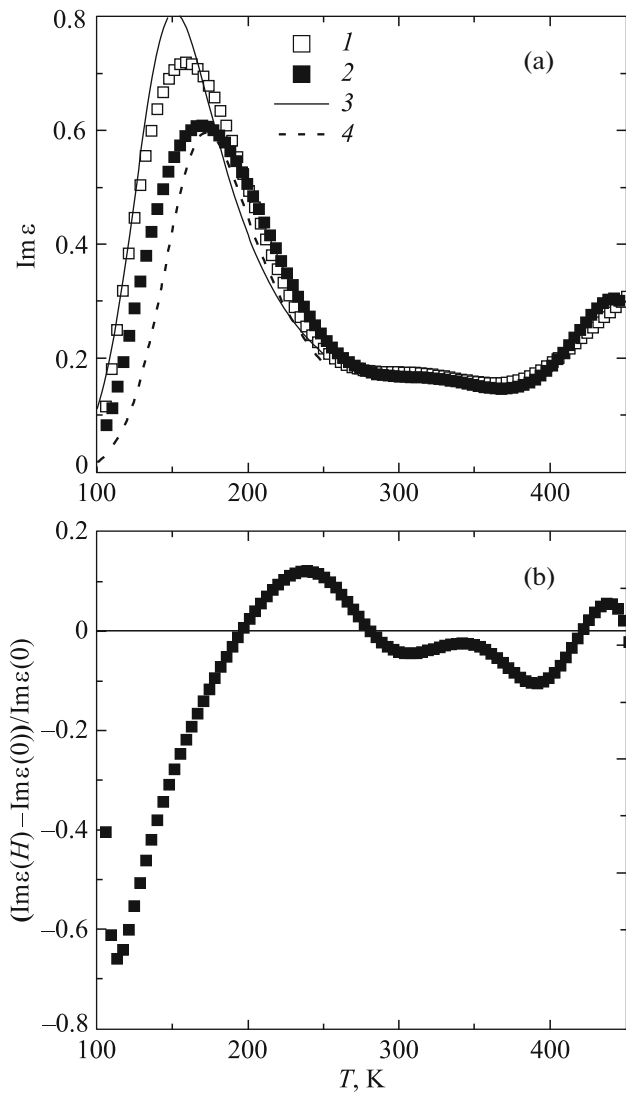


**Fig. 5.** (a) Temperature dependence of the imaginary part of the permittivity of the  $\text{Gd}_{0.2}\text{Mn}_{0.8}\text{S}$  solid solution, measured at a frequency of 10 kHz (1) without field and (2) in the magnetic field of 8 kOe. Approximating functions (formula (4)) with activation energies (3)  $\Delta E = 0.078$  eV without field and (4)  $\Delta E = 0.091$  eV in the magnetic field of 8 kOe. (b) Relative variation of the imaginary part of the permittivity in the magnetic field as a function of temperature. The values of parameters are the same as in panel (a).

ium subsystem. The dc conductivity varies in magnitude by a factor of 3 (Fig. 4b), and the imaginary part of the permittivity varies by an order of magnitude in the temperature range of 100–400 K (Fig. 5a). The temperature dependence of  $\text{Im}(\epsilon(\omega))$  has two maxima: at  $T = 157$  and 442 K. In the magnetic field  $H = 8$  kOe, the low-temperature maximum shifts to higher temperatures to  $T = 170$  K, the dielectric loss decreases in the magnetic field, except for the temperature ranges of 194–279 and 417–451 K (Fig. 5a). Let us describe the low-temperature maximum in the

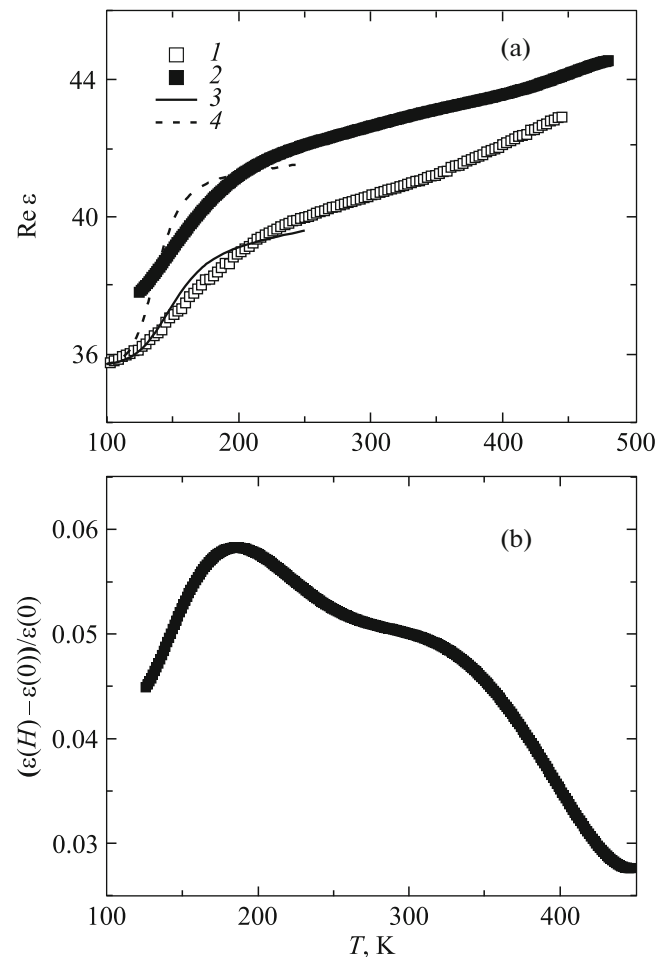


**Fig. 6.** (a) Real part of the permittivity of the  $\text{Gd}_{0.2}\text{Mn}_{0.8}\text{S}$  solid solution, measured at a frequency of 10 kHz (1) without field and (2) in the magnetic field  $H = 8$  kOe as a function of temperature. Approximating functions  $\text{Re} \epsilon = A/(1 + B \exp(2\Delta E/T)) + \epsilon_0$  with activation energies (3)  $\Delta E = 0.078$  eV for the permittivity without field and (4)  $\Delta E = 0.091$  eV for the permittivity in the magnetic field. (b) Magnetocapacitance in the magnetic field of 8 kOe as a function of temperature.

localized electron model (1) with freezing of dipole moments with the activation energy  $\Delta E = 0.078$  eV without magnetic field and with  $\Delta E = 0.091$  eV in the magnetic field. The approximating function

$$\text{Im} \epsilon = A_1 \exp(\Delta E/T) / (1 + B \exp(2\Delta E/T)) \quad (4)$$

describes well the experimental data in Fig. 5a in the temperature range of 100–250 K.

This maximum can be explained either by electric dipole reorientation or charge transfer between inequivalent sites in the material lattice, which is in a sense equivalent to electric dipole reorientation. The increase in the magnetoresistance in  $\text{Gd}_{0.2}\text{Mn}_{0.8}\text{S}$  [8] in the magnetic field disproves the version associated with charge transfer. The decrease in the dielectric loss in the magnetic field is associated with the electron

density redistribution over  $t_{2g}$ -orbitals, e.g., between  $d_{zx}$  and  $d_{zy}$ , which is equivalent to electric dipole turn rotation. Partial ordering of dipoles leads to increasing polarization. The position of the permittivity anomaly is caused by the characteristic relaxation time of the subsystem under consideration.

The real part of the permittivity is shown in Fig. 6. In the temperature range of 130–210 K, a sharp increase in the permittivity is observed. In the magnetic field  $H = 8$  kOe,  $\text{Re}(\epsilon(\omega))$  increases, and the relative change in the permittivity  $\delta\epsilon_H = (\epsilon(H, T) - \epsilon(0, T))/\epsilon(0, T)$  reaches a maximum of 6% at  $T = 184$  K. The sharp change in the permittivity with decreasing temperature is also described in the model of dipole moment freezing with the activation energy  $\Delta E = 0.078\text{--}0.091$  eV.

Thus, for the  $\text{Gd}_{0.04}\text{Mn}_{0.96}\text{S}$  composition, a sharp (stepwise) decrease in the permittivity at low temperatures was detected, which is associated with lattice structure distortion. As the gadolinium ion concentration increases, the low-temperature maximum of the imaginary part of the permittivity increases and shifts to the high-temperature region, as in the magnetic field. The decrease in the dielectric loss in the magnetic field is caused by the localized electron redistribution in  $t_{2g}$ -orbitals and the shift of the electron density maximum energy with respect to the chemical potential, which results in an increase in the activation energy. These results are well described in the Debye model with dipole moment freezing. The increase in the permittivity in the region above room temperature is caused by the increase in the electron delocalization length and the disappearance of orbital-charging ordering. The qualitative difference in the temperature behavior of the magnetocapacitance and magnetoresistance was detected, which is explained by localized and delocalized electrons.

#### ACKNOWLEDGMENTS

This study was supported by the Russian Foundation for Basic Research (project no. 15-42-04099 r\_si-

bir\_a) and the Ministry of Education and Science of the Russian Federation (state contract no. 114090470016).

#### REFERENCES

1. M. Fiebig, T. Löttermoser, D. Fröhlich, A. V. Goltsev, and R. V. Pisarev, *Nature (London)* **419**, 818 (2002).
2. A. P. Pyatakov and A. K. Zvezdin, *Phys.—Usp.* **55** (6), 557 (2012).
3. G. A. Smolenskii and I. E. Chupis, *Sov. Phys.—Usp.* **25** (7), 475 (1982).
4. S. S. Aplesnin, V. V. Kretinin, A. M. Panasevich, and K. I. Yanushkevich, *J. Exp. Theor. Phys.* **121** (3), 422 (2015).
5. N. Ikeda, H. Ohsumi, K. Ohwada, K. Ishii, T. Inami, K. Kakurai, Y. Murakami, K. Yoshii, S. Mori, Y. Horibe, and H. Kito, *Nature (London)* **436**, 1136 (2005).
6. A. Scaramucci, E. Bousquet, M. Fechner, M. Mostovoy, and N. A. Spaldin, *Phys. Rev. Lett.* **109**, 19 (2012).
7. J. P. Rivera and H. Schmid, *Ferroelectrics* **161**, 91 (1994).
8. S. S. Aplesnin and M. N. Sitnikov, *JETP Lett.* **100** (2), 95 (2014).
9. C. Aebischer, D. Baeriswyl, and R. M. Noack, *Phys. Rev. Lett.* **86**, 468 (2001).
10. J. Hemberger, P. Lunkenheimer, R. Fichtl, H. A. Krug von Nidda, V. Tsurkan, and A. Loidl, *Nature (London)* **434**, 364 (2005).
11. M. M. Parish and P. B. Littlewood, *Phys. Rev. Lett.* **101** (16), 166602 (2008).
12. P. Lunkenheimer, V. Bobnar, A. V. Pronin, A. I. Ritus, A. A. Volkov, and A. Loidl, *Phys. Rev. B: Condens. Matter* **66**, 052105 (2002).
13. G. Catalan, *Appl. Phys. Lett.* **88**, 102902 (2006).
14. S. S. Aplesnin, L. I. Ryabinkina, O. B. Romanova, V. V. Sokolov, A. Yu. Pichugin, A. I. Galyas, O. F. Demidenko, G. I. Makovetskii, and K. I. Yanushkevich, *Phys. Solid State* **51** (4), 698 (2009).
15. S. S. Aplesnin, *Magnetic and Electrical Properties of Strongly Correlated Magnetic Semiconductors with Four-Spin Coupling and Orbital Ordering* (Fizmatlit, Moscow, 2013) [in Russian].

*Translated by A. Kazantsev*